

# Mat lab/simulink based fault analysis of pv grid with intelligent fuzzy logic control mppt

Neeraj Priyadarshi<sup>1\*</sup>, Amarjeet Kr. Sharma<sup>1</sup>, Akash Kr. Bhoi<sup>2</sup>, S.N. Ahmad<sup>1</sup>, Farooque Azam<sup>1</sup>, S. Priyam<sup>1</sup>

<sup>1</sup> Millia Institute of Technology, Punea 854301, India

<sup>2</sup> Dept. of Electrical and Electronics Engineering, Sikkim Manipal Institute of Technology, SMU, Sikkim, INDIA-7371363

\*Corresponding author E-mail: neerajrd@gmail.com

## Abstract

This paper mainly presents the fault analysis of Photovoltaic (PV) grid power system. The fuzzy logic controller (FLC) based intelligent maximum power point tracking (MPPT) algorithm has been employed in this work. Moreover, the hysteresis controller has been implemented for inverter control. Simulation results based on MATLAB/SIMULINK justify the effectiveness of the proposed PV power system under different fault operating conditions.

**Keyword:** FLC; Hysteresis Controller; MATLAB; PV

## 1. Introduction

Because of continuous depletion of fossil fuels and energy security challenges, renewable energy sources are playing important role for production of electrical power. Photovoltaic (PV), wind energy, fuel cell, tidal energy, geothermal energy etc are the main renewable energy concern [1]-[3]. Compared to other renewable sources, the PV system is the most acceptable technology for electricity generation. As it has no moving parts and produce green and pollution free environment. However, because of high installation cost and low tracked efficiency, the maximum power point tracking (MPPT) technology has been added with PV power system [4]-[6]. Various MPPT algorithms have been used to improve the conversion efficiency of the PV module [7]. In view of this work fuzzy logic controller (FLC) based MPPT controller has been used to track the optimal power from PV modules [8]. Also, hysteresis controller for inverter current control strategy has been also employed [9]-[10]. The different faults L-G, L-L, LLL, LLG, and LLLG have been realized on grid side using MATLAB/SIMULINK environment.

### 1.1. Proposed structure of PV grid

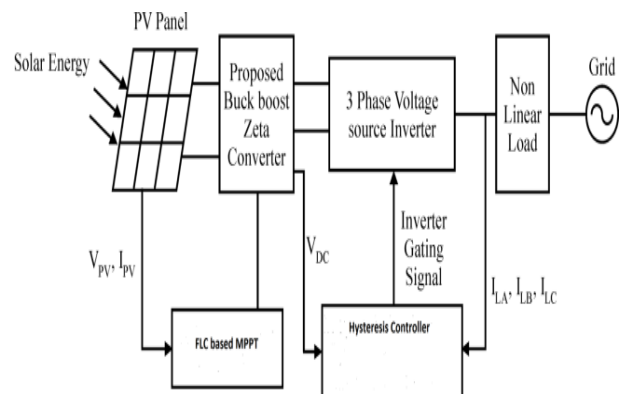


Fig. 1: Block Diagram of Proposed PV Power Circuit Based Utility Grid.

Fig 1.1 describes the structure of proposed PV grid with MPPT and inverter control. It comprises PV panel, buck-boost converter, inverter fed to the electric grid. The FLC based MPPT control is employed for buck boost converter. Hysteresis controller is also used to make sinusoidal inverter current for unity operated power factor.

### 1.2. Mathematical modeling of proposed zeta converter

State space model based zeta converter conducting in continuous mode is presented in this regard. Since zeta converter consists of two capacitors and two inductors and able to work in step down / up mode is called fourth order chopper which is depicted by Fig 1.2. With regard to the energy it acts as a buck converter, on the other hand with regard to the output it acts as a boost converter. The power circuit consists of capacitor and inductors as major elements which are employed for amplification and reduction of level of voltage. The complete operation is based on without polarity inversion and it acts as MPPT trackers which provide zero voltage ripple. Comparing to other dc-dc converters, it provides better voltage reg-

ulation, high tracked efficiency and reduction of stress level voltage. The main objective of maximum power point method is providing optimal PV power extraction. For maximizing the efficiency of buck-boost converter, the converters can be employed in continual conduction state. The supply voltage is same as system. Output  $V_s = V_{cs}$ , in the purpose of dynamicity.

$R_s$  and  $R_L$  represent the internal resistance of source and load respectively. The following assumptions are made for analysis:

- a) The converter operates in continuous inductor current mode.
- b) Switching devices should be real.
- c) DC voltage line frequency ripple is negligible

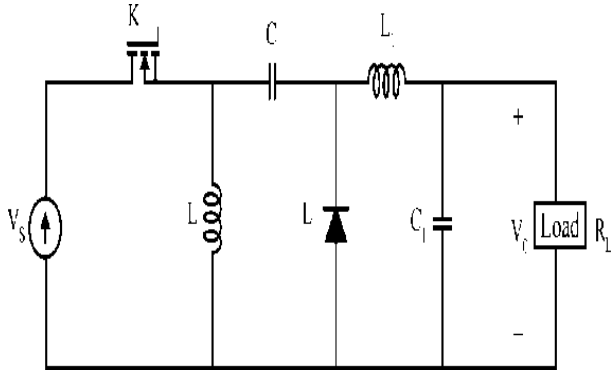


Fig. 2: Circuit Diagram of Zeta Converter.

Zeta converter is operating in two modes. In first, mode switch is opened and diode gets forward biased. The  $L_1$  energy stored can be transferred to  $R_L$ . Also, when switch is closed, the diode gets reverse biased and  $L$  and  $L_1$  currents are flowing through.

Equating average voltage across inductor,

$$DV_s = (1 - D) V_o$$

$$\Rightarrow \frac{V_o}{V_s} = \frac{D}{1 - D} \tag{1}$$

A. state space model of Zeta buck boost converter

Considering current is flowing through inductor  $I_L$  and voltage across capacitor  $V_C$  as a state variable. The average state space model for current fed zeta converter presented in Fig. 1.3 is expressed as:

$$\begin{bmatrix} \frac{dV_{Cs}}{dt} \\ \frac{dI_L}{dt} \\ \frac{dI_{L1}}{dt} \\ \frac{dV_C}{dt} \\ \frac{dV_{C1}}{dt} \end{bmatrix} = \begin{bmatrix} -\frac{1}{R_s C_s} & -\frac{1}{C_s} & 0 & 0 & 0 \\ \frac{d}{L} & 0 & 0 & -\frac{(1-D)}{L} & 0 \\ 0 & 0 & 0 & \frac{D}{L_1} & -\frac{1}{L_1} \\ 0 & -\frac{(1-D)}{C_1} & -\frac{D}{C_1} & 0 & 0 \\ 0 & -\frac{(1-D)}{C_1} & -\frac{(1-D)}{C_1} & 0 & -\frac{1}{R_L C_1} \end{bmatrix} \begin{bmatrix} V_{Cs} \\ I_L \\ I_{L1} \\ V_C \\ V_{C1} \end{bmatrix} + \begin{bmatrix} \frac{1}{C_s} \\ 0 \\ 0 \\ 0 \\ 0 \end{bmatrix} I_s$$

$$V_s = V_{cs}$$

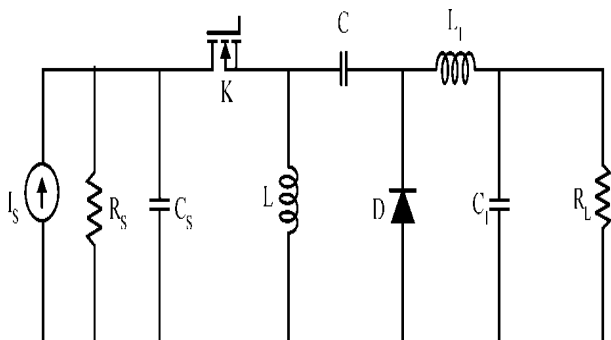


Fig. 3: Equivalent Circuit of Current Fed Zeta Converter.

Similarly, the small signal dynamic model is

$$\begin{bmatrix} \frac{d\tilde{V}_{Cs}}{dt} \\ \frac{d\tilde{I}_L}{dt} \\ \frac{d\tilde{I}_{L1}}{dt} \\ \frac{d\tilde{V}_C}{dt} \\ \frac{d\tilde{V}_{C1}}{dt} \end{bmatrix} = \begin{bmatrix} -\frac{1}{R_s C_s} & -\frac{1}{C_s} & 0 & 0 & 0 \\ \frac{d}{L} & 0 & 0 & -\frac{(1-\tilde{D})}{L} & 0 \\ 0 & 0 & 0 & \frac{\tilde{D}}{L_1} & -\frac{1}{L_1} \\ 0 & -\frac{(1-\tilde{D})}{C_1} & -\frac{\tilde{D}}{C_1} & 0 & 0 \\ 0 & 0 & -\frac{1}{C_1} & 0 & -\frac{1}{R_L C_1} \end{bmatrix} \begin{bmatrix} \tilde{V}_{Cs} \\ \tilde{I}_L \\ \tilde{I}_{L1} \\ \tilde{V}_C \\ \tilde{V}_{C1} \end{bmatrix} + \begin{bmatrix} 0 \\ \frac{\tilde{V}_C + \tilde{V}_{C1}}{L_1} + \frac{\tilde{I}_L}{L_1} \\ \frac{\tilde{V}_C + \tilde{V}_{C1}}{L_1} \\ -\frac{1}{C_1} \tilde{I}_L - \frac{1}{C_1} \tilde{I}_{L1} \\ 0 \end{bmatrix} \tilde{d}$$

$$\tilde{V}_s = \tilde{V}_{Cs}$$

### 1.3. Proposed adaptive fuzzy logic controller based mppt

Fig 1.4 presents the overall block diagram portrayed of the FLC controller which consists of fuzzification, rule base and defuzzification as the major components. PV voltage and current are sensed which acts as a crisp value to the fuzzification block. The fuzzification converts crisp value to fuzzy value. Inference rule base have been employed to take the fuzzy decisions. These rules are based on IF/THEN basis which comprises mamdani max-min composition. The fuzzy parameters can be converted into numerical value using defuzzification method in which centroid method is employed. The FLC controller using MATLAB can be constructed and presented by Fig 1.5.

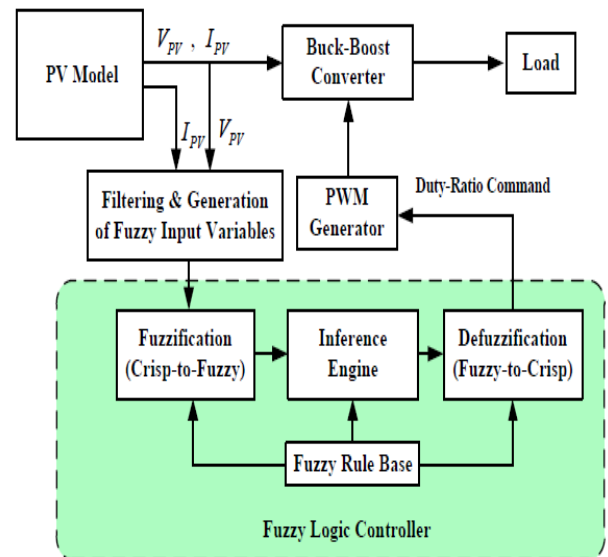


Fig. 4: FLC Structure.

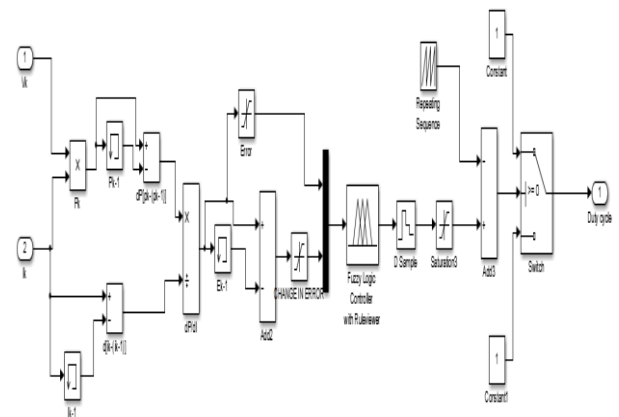


Fig.5: Flc Using Matlab/Simulink.

### 1.4. Hysteresis inverter control

In this paper hysteresis based non-linear inverter control has been employed for generation of switching pulses. In this method instantaneous reactive power has been used to produce inverter reference current. The 3-phase voltage and load currents have been transformed using clark's transformation from a-b-c to  $\alpha$ - $\beta$ -0 frame. Using this transformation, reference current has been generated which acts as an input to hysteresis controller. Fig 1.6 depicts the hysteresis controller using SIMULINK. Generation of the reference current using MATLAB/SIMULINK is explained by Fig 1.7.

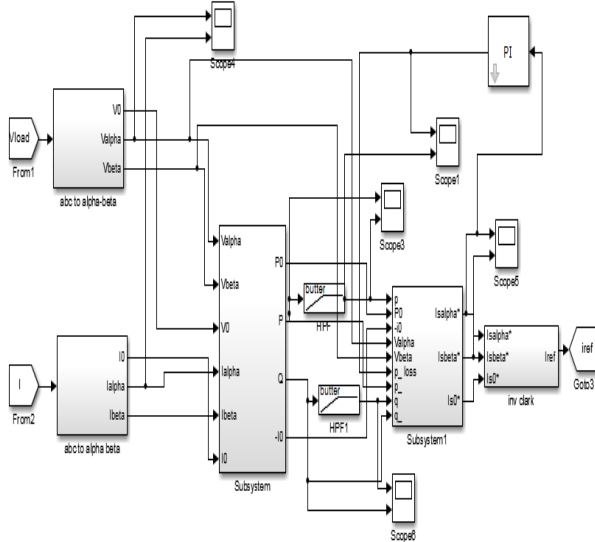


Fig. 6: Hysteresis Current Control Using Matlab/Simulink.

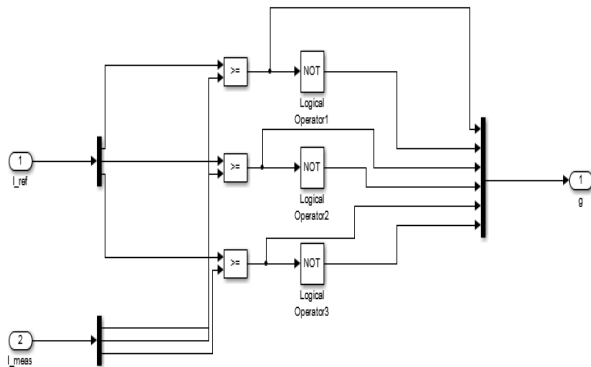


Fig.7: Generation of the Reference Current Using MATLAB/SIMULINK.

## 2. Response during system fault condition

Several faults have been created on grid side and total harmonic distortion (THD) has been analyzed. Fig 8 describes the MATLAB/Simulink based grid connected power system. The proposed system has been analyzed on 1000 W/m<sup>2</sup> irradiance with 25<sup>o</sup> C ambient temperature. Duration of fault is of 0.2 sec. The grid voltage, grid current, inverter current, active and reactive power with inverter current FFT have been studied. The proposed PV power system has been simulated under without and with fault conditions.

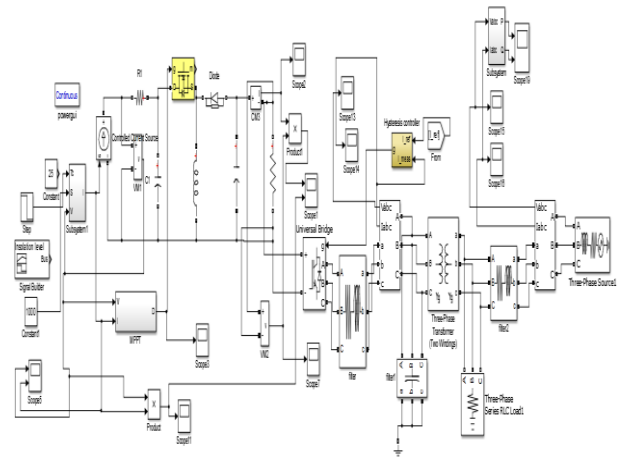
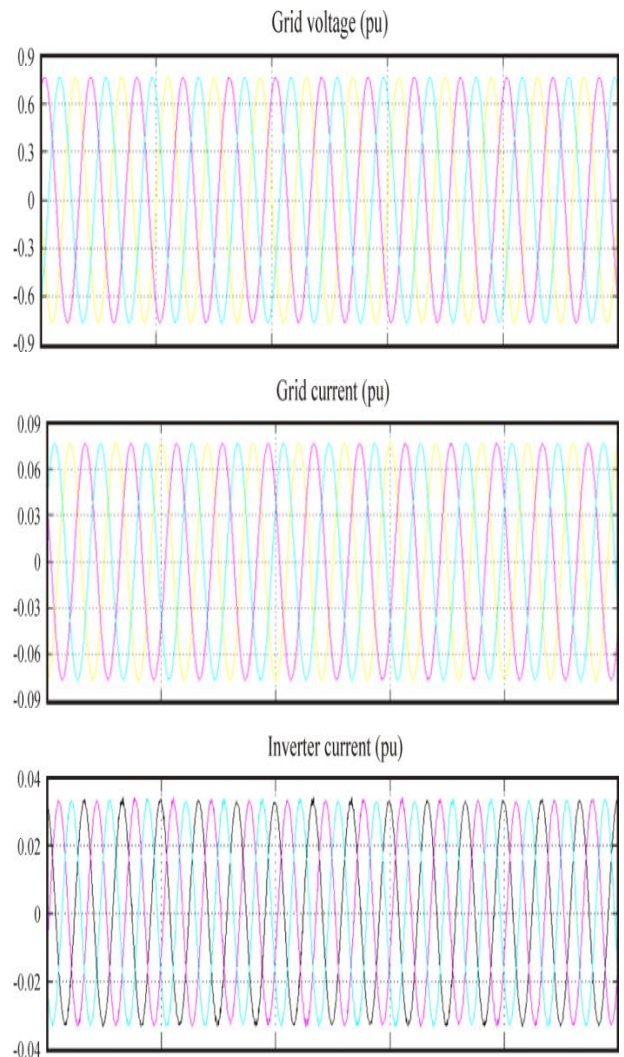
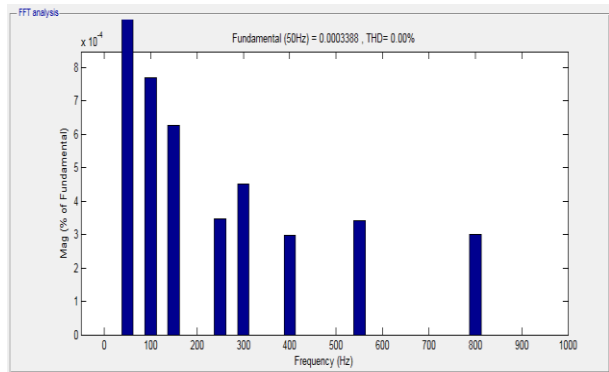
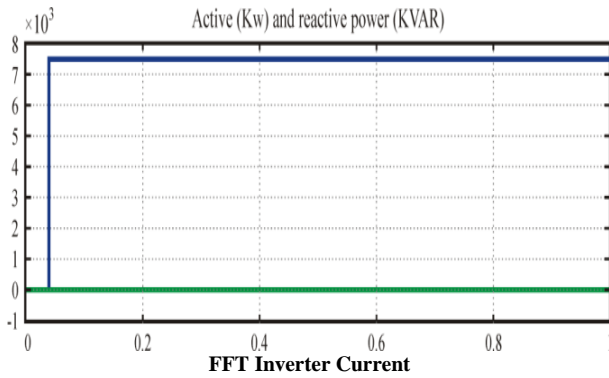


Fig.8: MATLAB/Simulink Based Grid Connected Power System.

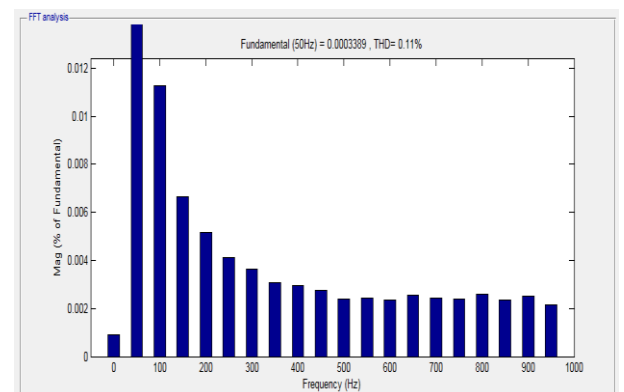
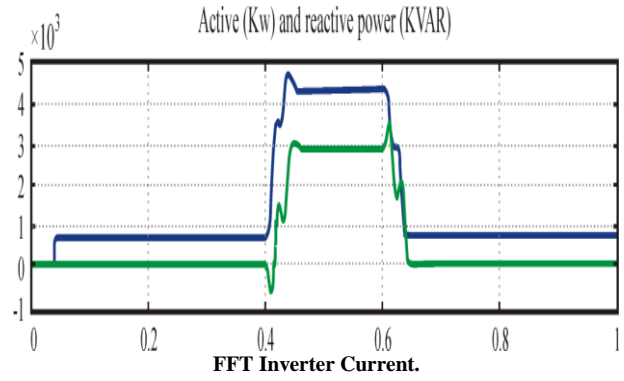
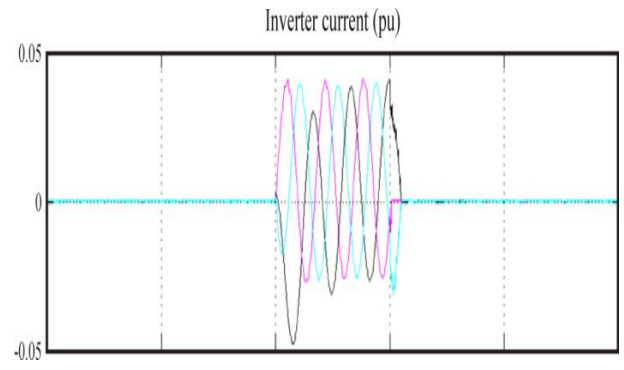
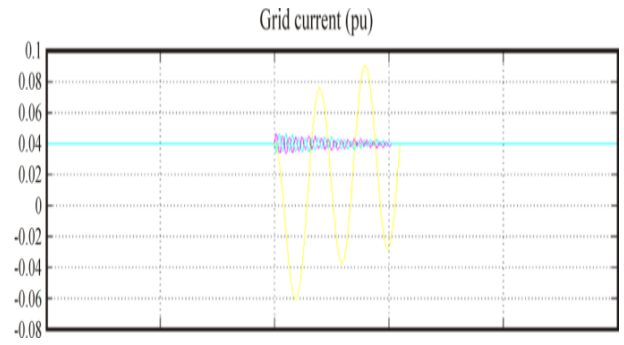
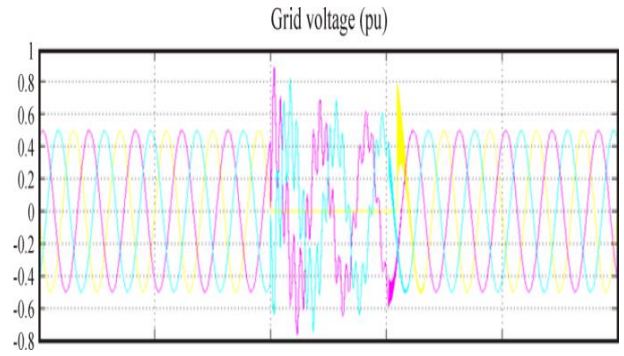
The grid side fault can be generated for 0.2 sec from 0.4 to 0.6 seconds. The Fig. 9 shows various waveforms without Fault condition. The complete system behavior can be extensively analyzed under without fault and with fault conditions viz. three phase LG, LL, LLG, LLL and LLLG faulty conditions. The waveforms of grid voltage, grid current, inverter current, FFT inverter current and grid side active and reactive power have been found at different fault conditions.



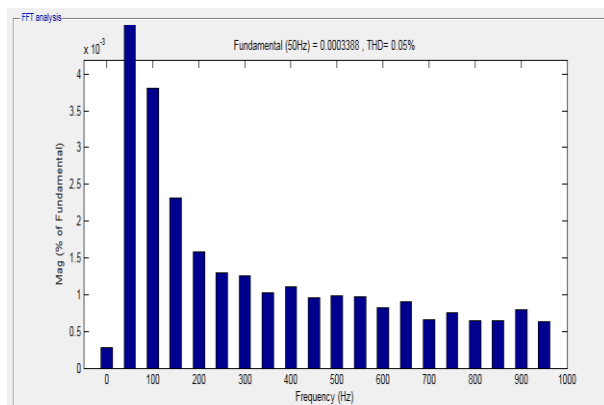
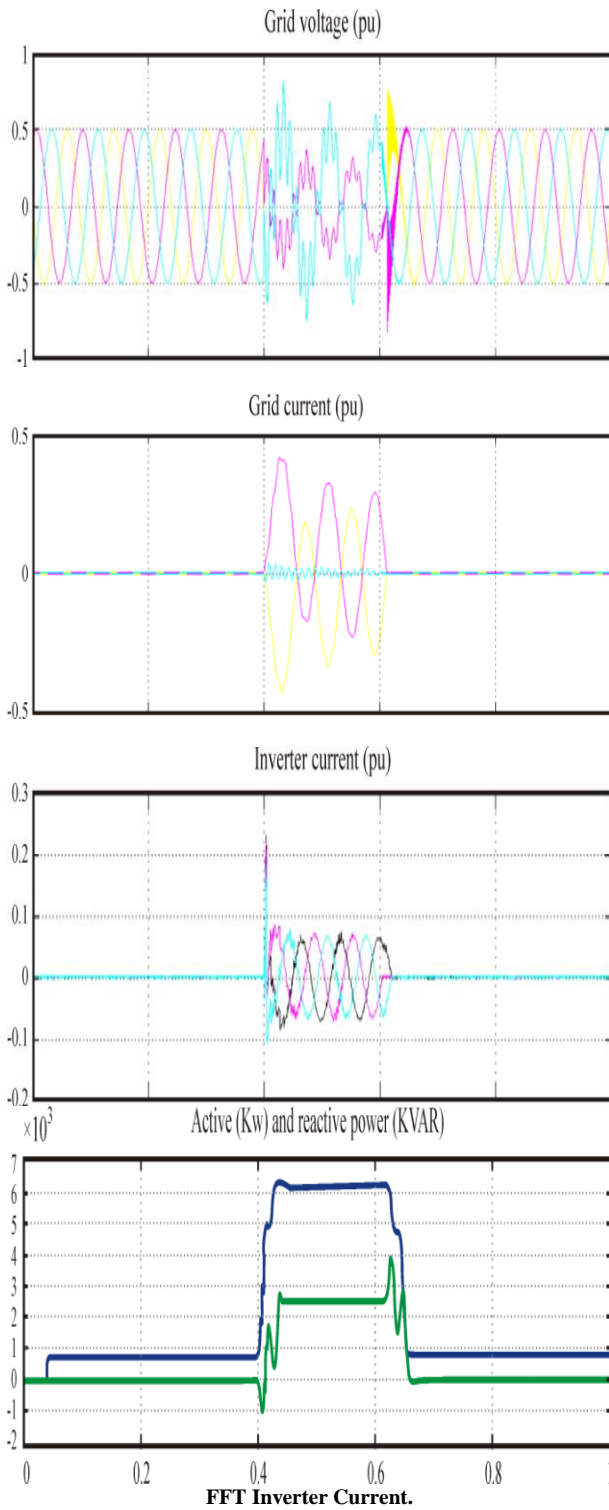


**Fig. 9:** Simulated Responses without Fault Condition. Grid Voltage, Grid Current, Inverter Current, Active and Reactive Power Grid Side, FFT Inverter Current.

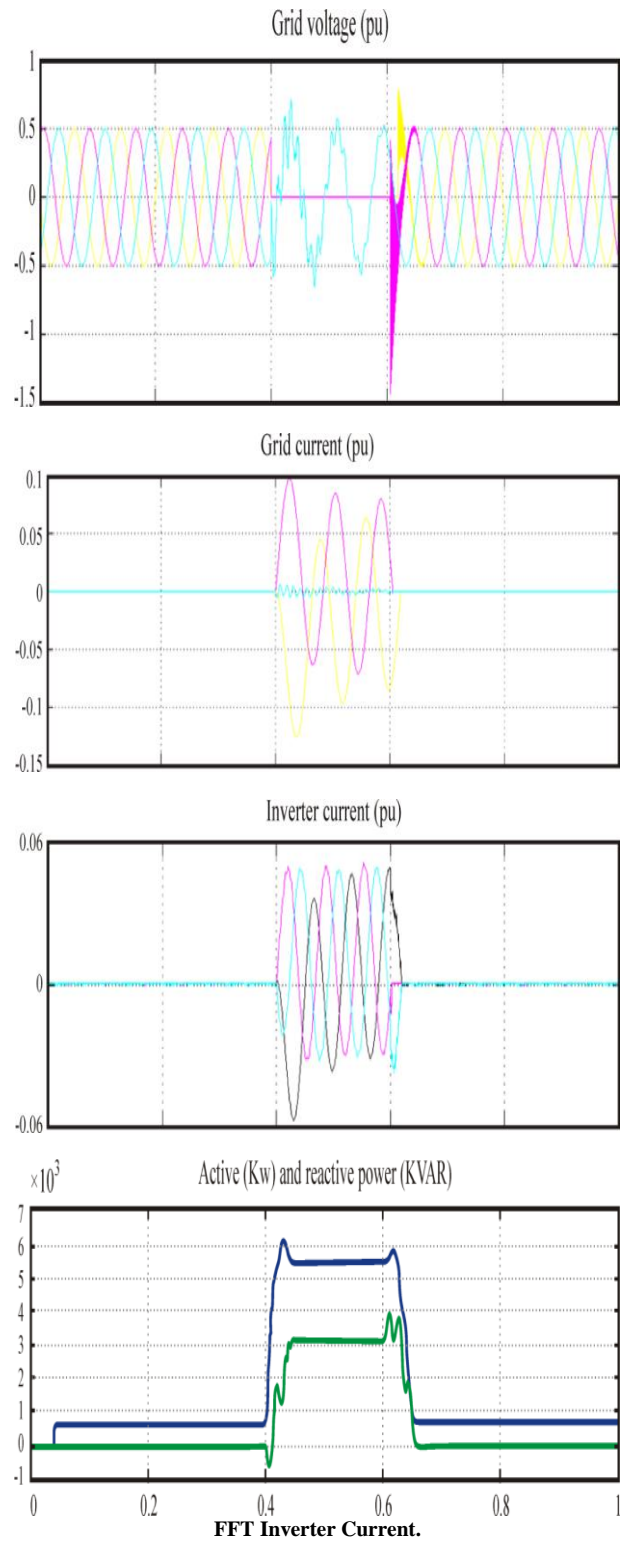
The proposed system is studied without fault condition and the corresponding variation in grid voltage, inverter current and grid currents are shown in Fig. 1.9. From FFT analysis the inverter current has total harmonic distortion 0.00%. When a three phase LG fault occurs in the proposed system on grid side the corresponding variation in grid voltage, inverter current and grid currents are shown in Fig. 1.10. The fault is initiated at 0.4 sec, while cleared at 0.6 sec. In case of emergency condition a 3 phase circuit breaker is connected to the grid side to isolate the PV generation system from the distribution system. From FFT analysis the inverter current has total harmonic distortion 0.11%. When a three phase LL fault occurs in the proposed system on grid side the corresponding variation in grid voltage, inverter current and grid currents are shown in Fig 1.11. The fault is initiated at 0.4 sec, while cleared at 0.6 sec. Under LL fault, the amplitude of grid current is shown in simulated results. From FFT analysis the inverter current has total harmonic distortion 0.05%. When a three phase LLL fault occurs in the proposed system on grid side the corresponding variation in grid voltage, inverter current and grid currents are shown in Fig 1.12. The fault is initiated at 0.4 sec, while cleared at 0.6 sec. During line to ground fault period, the magnitude of grid current increases as shown in simulated results. From FFT analysis the inverter current has total harmonic distortion 0.10%. When a three phase LLLG fault occurs in the proposed system on grid side the corresponding variation in grid voltage, inverter current and grid currents are shown in Fig. 1.13. The fault is initiated at 0.4 sec., while cleared at 0.6 sec. During line to ground fault period, the magnitude of grid current increases as shown in simulated results. From FFT analysis the inverter current has total harmonic distortion 0.03%. During three phase LLLG fault the magnitude of grid current increases as shown in Fig. 1.14. From FFT analysis the inverter current has total harmonic distortion 0.06%. When LLLG Fault occurs in the proposed system on grid side the corresponding variation in grid voltage, inverter current and grid currents are shown in simulated results. The fault is initiated at 0.4 sec., while cleared at 0.6 sec.

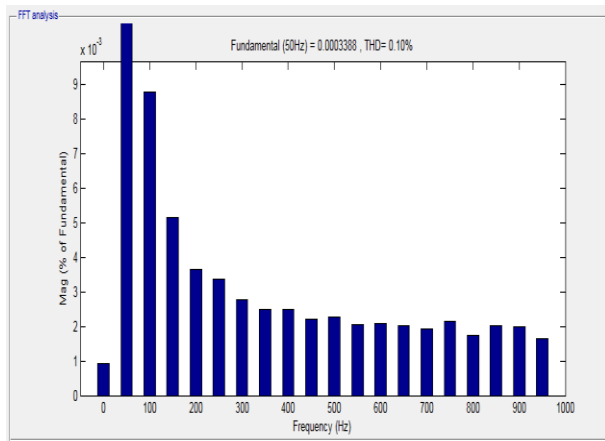


**Fig. 10:** Simulated Responses during LG Fault Condition. Grid Voltage, Grid Current, Inverter Current, Active and Reactive Power Grid Side, FFT Inverter Current.

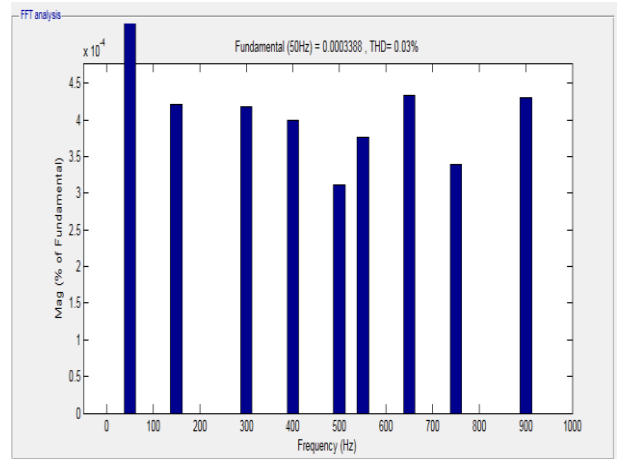
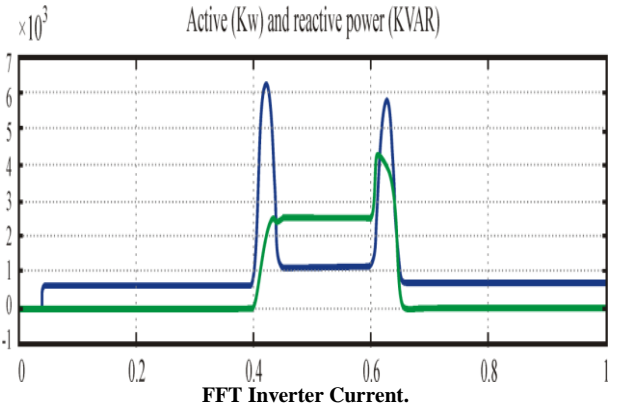
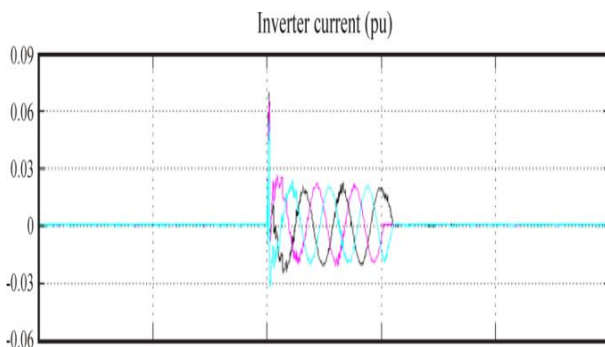
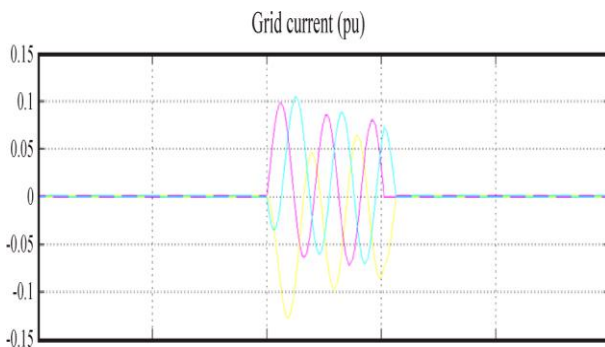
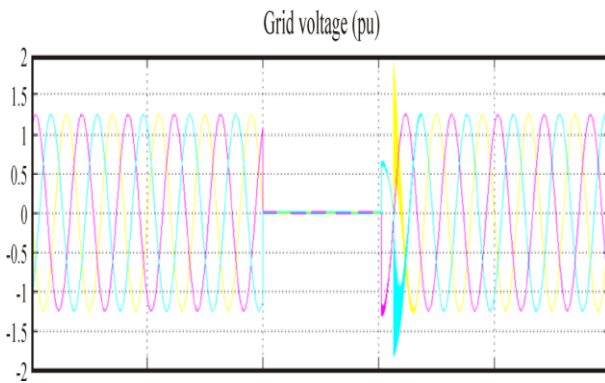


**Fig. 11:** Simulated Responses during LL Fault Condition. Grid Voltage, Grid Current, Inverter Current, Active and Reactive Power Grid Side, FFT Inverter Current

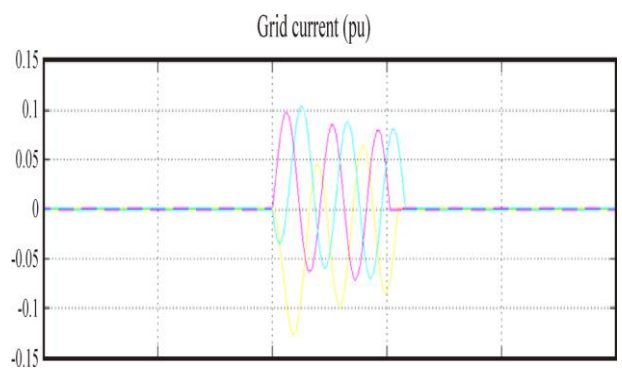
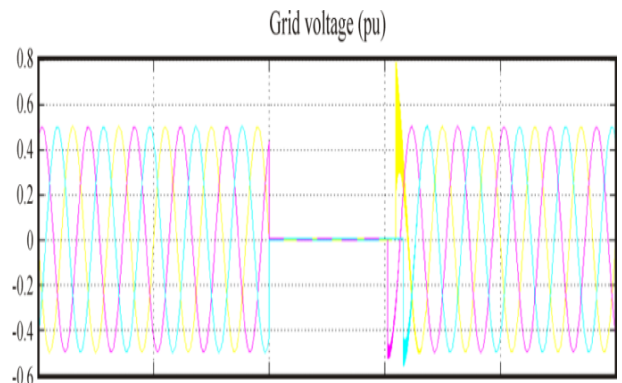




**Fig. 12:** Simulated Responses during LLG Fault Condition Grid Voltage, Grid Current, Inverter Current, Active and Reactive Power Grid Side, FFT Inverter Current



**Fig. 13:** Simulated Responses during LLL Fault Condition. Grid Voltage, Grid Current, Inverter Current, Active and Reactive Power Grid Side, FFT Inverter Current.



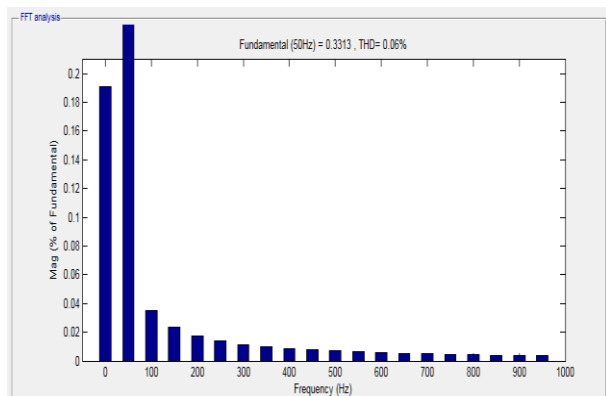
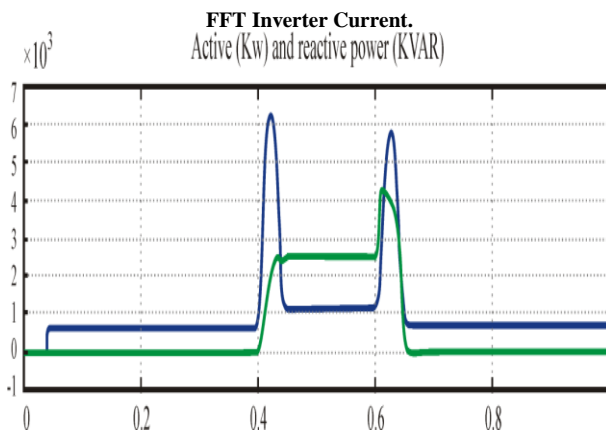
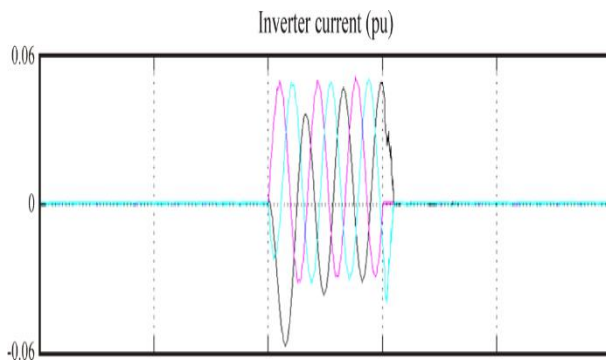


Fig. 14: Simulated Responses during LLLG Fault Condition. Grid Voltage, Grid Current, Inverter Current, Active and Reactive Power Grid Side, FFT Inverter Current

### 3. Power circuit structure

PV power circuit model for grid utility was built with protection circuitry and necessary control. Between PV module and three phase inverter, zeta converter works as an interface. The power circuit block diagram has been illustrated in Fig. 1.15.

### 4. Conclusion

This paper describes the various fault analysis for grid PV power system. Simulated results explain that within 0.2 sec, the proposed power system gains stability at normal frequency. The different fault on grid side has been analyzed for proper design of protection circuit. The MPPT and inverter control strategies for PV power system are working efficiently.

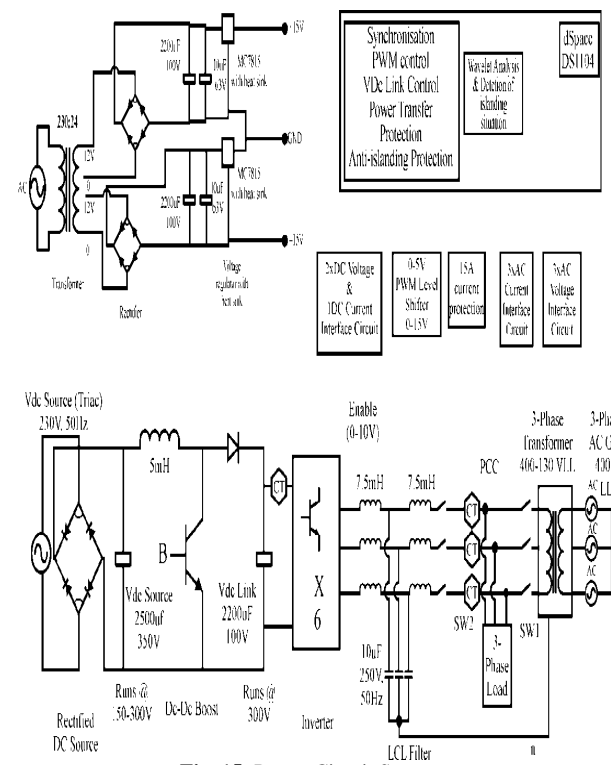


Fig. 15: Power Circuit Structure.

### References

- [1] M.I. Munir, T. Aldhanhani and K.H. Al Hosani, "Control of Grid Connected PV Array using P&O MPPT Algorithm," Ninth Annual IEEE Green Technologies Conference, pp. 52-58 (2017).
- [2] A. Sandali and A. Cherit, "New Adapted Forms of P-V Optimal Slope MPPT for a Better Grid Connected PV System Integration," IEEE International Conference on Industrial Technology (ICIT), pp. 446-451 (2017).
- [3] A. Ambikapathy, G. Singh and A. Shrivastava, "Efficient Soft-Switching dc-dc converter for MPPT of a Grid Connected PV System," International Conference on Computing, Communication and Automation (ICCCA2016), pp. 934-938. (2016).
- [4] M. Srivastava and A. Saxena, "Direct and Quadrature Axis Voltage and Current Control of a Three Phase Grid Connected PV System with Adaptive Fuzzy Logic MPPT Controller," 1st IEEE International Conference on Power Electronics, Intelligent Control and Energy Systems (ICPEICES-2016), pp.1-5. (2016).
- [5] N. Priyadarshi, A. Anand, A.K. Sharma, F. Azam, V.K. Singh, and R.K. Sinha, "An Experimental Implementation and Testing of GA based Maximum Power Point Tracking for PV System under Varying Ambient Conditions Using dSPACE DS 1104 Controller", International Journal Of Renewable Energy Research, Vol.7, No.1, pp. 255-265, 2017.
- [6] M. Ali, F. Usman, A. Yousof, "Design and Simulation of Power Electronic Controller for Grid Connected PV Array with Maximum Power Point Tracking (MPPT)," The 8th International Renewable Energy Congress (IREC 2017),
- [7] A. Saidi, C. Benachaiba, "Comparison of IC and P&O algorithm for grid connected PV module. 8th International Conference on Modelling, Identification and Control (ICMIC), pp. 213-218. (2016).
- [8] N. Priyadarshi, V. Kumar, K. Yadav, and M. Vardia, "An Experimental Study on Zeta buck-boost converter for Application in PV system," Handbook of distributed generation (Springer) chapter DOI 10.1007/978-3-319-51343-0\_13.
- [9] B. Chokkalingam, S.K. Padmanaban, P. Siano, Z. Leonowicz and Al. Iqba, "A Hexagonal Hysteresis Space Vector Current Controller for Single Z-Source Network Multilevel Inverter with Capacitor Balancing," IEEE International Conference on Environment and Electrical Engineering and 2017 IEEE Industrial and Commercial Power Systems Europe (EEEIC / I&CPS Europe), pp. 1-6. (2016)
- [10] Poonia, A., Dey, "Space Phasor based Improved Hysteresis Current Controller for Shunt Active Power Filter using 3-Level Inverter," 18th European Conference on Power Electronics and Applications (EPE'16 ECCE Europe), pp.1-10. (2016).